Applied Catalysis A: General 471 (2014) 84–90

Contents lists available at ScienceDirect

Applied Catalysis A: General

journal homepage: www.elsevier.com/locate/apcata

A comparative study on the effect of Zn addition to Cu/Ce and Cu/Ce–Al catalysts in the steam reforming of methanol

Mary Mrad[a,b], Dima Hammoud[a,b,c], Cédric Gennequin[a,b,*], Antoine Aboukaïs[a,b], Edmond Abi-Aad[a,b]

[a] Université Lille Nord de France, F-59000 Lille, France
[b] Université du Littoral Cote d'Opale, Unité de Chimie Environnementale et Interaction sur le Vivant, E.A. 4492, MREI 1, 145 avenue Maurice Schumann, 59140 Dunkerque, France
[c] Conseil National de la Recherche Scientifique, Beyrouth, République Libanaise

ARTICLE INFO

Article history:
Received 13 June 2013
Received in revised form 8 November 2013
Accepted 21 November 2013
Available online 1 December 2013

Keywords:
Hydrogen
Steam reforming of methanol
Copper and zinc catalysts

ABSTRACT

The performances of different catalysts *x*Cu10Ce and *x*Cu10Ce10Al (with $x = 1$, 3 and 5) in the steam reforming of methanol reaction were studied with and without the presence of zinc. The reaction was investigated at 350 °C with a Gas Hourly Space Velocity of 15,500 h^{-1} and a steamed mixture of water and methanol ($H_2O/CH_3OH = 2$). The catalytic activity was found to be strongly dependent on the nature of the copper species present on the support and on the nature of the support. The addition of ZnO is beneficial to the solid 5Cu10Ce and promotes interaction between Cu—Ce—O eventually leading to the reduction of Cu^{2+} to Cu^{+} and Cu^{0} the most active species in the SRM reaction.

1. Introduction

Recent studies reveal a fast increase of the greenhouse gas emission [1,2]. Although the high cost of fossil fuels, the traffic pollution expands. In order to produce clean energy it is necessary to develop fuel cells technology as an alternative energy model. With their high efficiency and their low emission label, fuel cells are presented as suitable power sources for automotive applications [2]. Hydrogen has been envisaged to be the ideal clean energy vector in the future and its performance is developed in fuel cells usage [3]. The direct use of hydrogen for fuel cell application is hindered by problems of supply, safety storage and handling. These problems can be resolved by using a suitable high energy/density liquid fuel, such as methanol as a hydrogen carrier. Methanol can be produced from renewable sources and is known for its low cost and high H:C ratio [4]. Hydrogen could be obtained through different reforming process. One interesting method is hydrogen production from methanol via steam reforming (SRM (1)) [5]. It is a process that occurs at moderate temperatures (200–400 °C) and can provide a product gas with high hydrogen content (up to 75%) and low CO concentration (1–2%) [6].

$$CH_3OH + H_2O \rightarrow 3H_2 + CO_2, \qquad \Delta H^{\circ} = +49.4\ kJ\ mol^{-1} \qquad (1)$$

Many researches have been focused on the CuO/CeO_2 mixed oxide, because of the low cost of the base metal compared to the precious metals and the high catalytic efficiency of this catalyst for various reactions [7,8]. Oxygen's high mobility and the strong metal-support interaction make the CeO_2 based materials very interesting for catalysis [9]. Copper-based catalysts are widely used for generating hydrogen from methanol [10–12]. It was shown that the interaction between copper and ceria plays an important role in promoting the catalytic activity [13]. Alumina is also considered as a promoter that increases the surface area and the thermal stability of Cu^0 [14]. The present work focuses on a comparative investigation of copper-containing catalysts supported on ceria or ceria/alumina in SRM and the influence before and after the addition of zinc. Physico-chemical analysis such as EPR, TPR, XRD, N_2O chemisorption are used to evaluate the influence of the copper loading, the dispersion of copper species on different supports, the support nature and the zinc effect on the methanol steam reforming reaction.

2. Experimental

2.1. Catalyst preparation

Cerium hydroxide $Ce(OH)_4$ was prepared as mentionned in a previous paper [15]. Then the deposition of copper was performed

* Corresponding author at: Université Lille Nord de France, F-59000 Lille, France/Université du Littoral Cote d'Opale, UCEIV EA 4492, F-59140 Dunkerque, France. Tel.: +33 3 28 65 82 62; fax: +33 3 2865 82 39.
E-mail address: cedric.gennequin@univ-littoral.fr (C. Gennequin).

0926-860X/$ – see front matter © 2013 Elsevier B.V. All rights reserved.
http://dx.doi.org/10.1016/j.apcata.2013.11.025

Table 1
Methanol conversion, activity, gas product composition and carbon assessment for methanol steam reforming over CeO_2, 10Ce10Al, *x*Cu10Ce, *x*Cu10Ce10Al, 5%Zn5Cu10Ce and 5%Zn5Cu10Ce10Al catalysts.

Sample	Methanol conversion (%)	Activity (10^{-4}) (mol min^{-1} g^{-1})	Product composition (%)				Carbon assessment	HCHO (10^{-4} mol)	CH_3OCHO (10^{-4} mol)
			H_2	CO_2	CO	CH_4			
CeO_2	65	4.70	92.5	7.5	0	0	0.45	–	–
10Ce10Al	82	8.69	90.2	0.0	9.4	0.4	0.35	–	116.631
1Cu10Ce10Al	98	9.75	75.7	24.2	0.1	0.0	0.98	–	176.621
3Cu10Ce10Al	98	8.5	74.9	25.0	0.1	0.0	0.98	–	162.412
5Cu10Ce10Al	99.8	10.0	75.0	25.0	0.0	0.0	0.98	–	146.105
5%Zn5Cu10Ce10Al	**96**	**9.33**	**74.9**	**25.0**	**0.1**	**0.0**	**0.73**	–	**28.23**
1Cu10Ce	98	5.2	75.6	23.8	0.1	0.5	0.89	2.091	–
3Cu10Ce	99.7	5.26	75.3	24.4	0	0.3	0.89	2.015	–
5Cu10Ce	99.7	5.3	75.1	24.9	0	0	0.96	1.042	–
5%Zn5Cu10Ce	**99.9**	**4.2**	**75**	**25**	**0**	**0**	**0.99**	–	–
Thermodynamics equilibrium at 350 °C for SRM reaction with the same conditions [a]	**97**	–	**75**	**25**	**0**	**0**	**1**	–	–

[a] Conditions of tests: these solids were pelletized and sieved to obtain catalysts with defined particle size in the range of $0.35 < d_p < 0.80$ mm; 0.2 cm^3 of catalyst was used; H_2O/CH_3OH ratio = 2 and GHSV = 15,500 h^{-1}; temperature is 350 °C.

by the impregnation onto the $Ce(OH)_4$ of an aqueous solution with given amounts of $Cu(NO_3)_2$ to obtain catalysts *x*Cu10Ce with different molar ratios (*x*/10) and *x* = 1, 3 and 5 [16]. Alumina (Al_2O_3) was prepared by sol–gel method, as mentionned [17]. The deposition of ceria was performed by the impregnation of an aqueous solution containing given amounts of $Ce(NO_3)_3$ onto the calcined Al_2O_3, to obtain catalysts 10Ce10Al. After drying at 100 °C for 20 h, the 10Ce10Al solid was calcined under air at 600 °C for 4 h. An aqueous solution containing a given amount of $Cu(NO_3)_2$ was also impregnated over the calcined 10Ce10Al as a support to obtain *x*Cu10Ce10Al with different molar ratios (with *x*/10: molar ratio and *x* = 1, 3 and 5) (Table 1). Then another impregnation of zinc (II) nitrate ($Zn(NO_3)_2$ was added over the 5Cu10Ce and 5Cu10Ce10Al prepared catalysts in order to obtain 5%Zn5Cu10Ce and 5%Zn5Cu10Ce10Al respectively. All the prepared solids were dried overnight and calcined under air at 600 °C for 4 h. These solids were pelletized and sieved to obtain catalysts with defined particle size, in the range of $0.35 < d_p < 0.80$ mm in order to eliminate mass transport limitation of the reaction rate.

2.2. Catalytic tests

Steam reforming of methanol was carried out in a quartz tubular fixed bed reactor with an inner diameter value of 8 mm at atmospheric pressure. The catalytic tests were realized at different isothermal temperatures, and in this paper we only present the results of tests performed during an isotherme of 350 °C for 5H. The measurement of the temperature is taken at the catalytic bed.

The catalytic test was carried out in the microflow reactor, which is assembled with a quartz EPR tube to allow the introduction of the catalyst into the resonance cavity without exposure to air. All runs were performed using 0.2 cm^3 of catalyst under an argon flow rate of 26 cm^3 min^{-1} (GHSV = 15,500 h^{-1}). The catalysts were not reduced under H_2 but pretreated under an argon flow at 350 °C for 12 h before test.

The composition of the liquid feed to the reactor was 0.8 cm^3 h^{-1} of water + methanol mixture (H_2O/CH_3OH = 2) evaporated with a heating filament at 150 °C before its introduction into the reactor. The product stream mixture was the passed through a chilled condenser to trap any unreacted water and methanol and possible condensable by-products. The mixture of dry gases effluent was analyzed on-line by a gas chromatograph (GC-Varian 3800) equipped with a Thermal Conductivity Detector (TCD) and a Flame Ionization Detector (FID).

The conditions of test are the same for all catalysts and the catalytic activity was evaluated in terms of conversion of methanol. The calculation of the conversion and activity are presented by the following formulas:

$$\text{Conversion}\,(\%) = 100 * \frac{n^0_{\text{MeOH}} - n^f_{\text{MeOH}}}{n^0_{\text{MeOH}}} \quad (2)$$

where n^0_{MeOH}, number of moles of injected methanol; n^f_{MeOH}, number of moles of none reacted methanol.

$$\text{Activity} = \frac{\text{Conversion} * D}{m} \quad (3)$$

D = flow in mol min^{-1} and *m* = mass in g.

After the test, the liquid fraction was placed in vials heated at 80 °C and injected via head space method (Varian GENESIS Head-Space) and analyzed by gas chromatograph (GC-Varian STAR 3400) equipped with a Flame Ionization Detector (FID). Also, the catalysts were also placed in vials and analyzed via head space method (Varian GENESIS Head-Space) equiped with a mass spectroscopy (HS–GC–MS). This allows us to identify the by-products condensed in the liquid fraction and adsorbed over the catalysts. The results reported are based on reactant conversions and selectivities to carbon-containing products for each catalyst. The carbon assessment (4) in Table 1 presents a calculation form of the ratio between the quantities of carbon presented in the products issued from the SRM reaction as gases (CO, CO_2 and CH_4) and as liquid fraction (non reacted part of methanol and carbonated by-products) and the carbon used as a reactant to feed the SRM reaction (initially introduced methanol). The ratio must be equal to 1 and the difference represents the adsorbed carbonate, the by-products and the coke formed over the catalysts during the test.

$$\text{Carbon assessment} = \frac{n_{\text{Total}_1} + n_{\text{Total}_2}}{n^0_{\text{MeOH}}} \quad (4)$$

where n^0_{MeOH}, number of moles of injected methanol; $n_{\text{Total}_1} = n_{CO_2} + n_{CO} + n_{CH_4}$ (total number of carbon recovered in gaseous form); n_{Total_2}, number of moles of carbon in liquid condensate.

2.3. Catalysts characterization

The Electron Paramagnetic Resonance (EPR) measurements are performed at room temperature and at −196 °C on an EMX BRUKER spectrometer with a cavity operating at a frequency of ∼9.5 GHz (X band). The magnetic field was modulated at 100 kHz and the power supply was sufficiently small to avoid saturation effect.

Modulation amplitudes from 0.5 to 10 Gauss were used. The g-values were determined using the relation: $h\nu = g\beta H$ where h is the Planck constant, β is the Bohr magneton, H the magnetic field and ν the microwave frequency measured with high precision using a frequency-meter. The relative EPR intensity is given, in arbitrary unit, by the normalized double integration of the EPR signal using BRUKER WINEPR program.

The structures of the solids were analyzed by powder X-ray Diffraction (XRD) technique at room temperature with a Bruker diffractometer using Cu Kα as radiation scanning (1.5406 Å) and 2θ angles ranging from 10 to 80° with a step size of 0.02° and a count time of 2 s.

Temperature Programmed Reduction (TPR) was carried out with a flow type reactor using a Zeton Altamira apparatus. Hydrogen (5 vol.% in Ar) was passed through a reaction tube containing the calcined catalyst under atmospheric pressure at 30 cm^3 min^{-1}. The TPR reactor was heated from ambient to 900 °C with an electric furnace at 5 °C min^{-1}, and the amount of H_2 consumed was monitored by a thermal conductivity detector (TCD).

Prior the TPR experiments, samples (30 mg) were activated under argon (30 mL min^{-1}) at 150 °C during 1H.

Copper dispersions were analyzed with a Zeton Altamira apparatus equipped with a quartz reactor. Before analysis, a pre reduction of the CuO to Cu was performed at 700 °C in a flowing H_2/Ar mixture, and then it was followed by an oxidation under a continuous flow of N_2O/Ar at 90 °C. After that, a second reduction of Cu_2O surface to Cu was carried out. The following formula is used to calculate the dispersion: $D = 2^*(A_2/A_1)^*100$ with A_1 and A_2 are the peak areas of first and second reduction respectively.

3. Results and discussion

3.1. Test results

Test results of the steam reforming of methanol reaction of all the prepared catalysts are shown in Table 1. All the catalysts were performed under the experimental conditions cited in Section 2.2. The CeO_2 support tested alone shows a relatively low methanol conversion (65%) and low activity.

A high selectivity of H_2 was obtained (92.5%) although it should not exceed 75% in steam reforming. Low CO_2 selectivity is also observed (7.5%). Differences are observed between the experimental and the theoretical results. 75% of H_2 and 25% of CO_2 are theoretically obtained for 97% conversion of methanol at 350 °C by the thermodynamics equilibrium. These results reveal that unfavorable reactions such as methanol decomposition have strong influence on the performance of the reforming reaction and contribute to the reactants consumption (Table 1).

As for the 10Ce10Al support, the methanol conversion and the activity show higher values than that shown for the ceria tested alone, this could be explained by the influence of the alumina addition that induces the increase of the surface specific area. In addition, a high selectivity of H_2 (90.2%) is also shown for the 10Ce10Al with the presence of CO (9.4%) and without any formation of CO_2, also 0.4% of CH_4 is detected.

By adding copper to 10Ce10Al, the conversion rate increases from 82% to 99.8% for 5Cu10Ce10Al and the steam reforming of methanol reaction seems to be enhanced without any formation of CH_4. The relatively low CO formation (0.1%) observed over 1Cu10Ce10Al and 3Cu10Ce10Al, disappears for the 5Cu10Ce10Al catalyst. The H_2 formation reaches the 75% for the 5Cu10Ce10Al respecting the stoichiometry of the steam reforming reaction without any formation of CO and CH_4. The increasing carbon assessment, after adding copper to the 10Ce10Al support, from 0.35 to 0.98, highlights the absence of carbon species over the copper supported catalysts. Otherwise, by increasing the copper content, the catalytic activity (10^{-3} mol min^{-1} g^{-1}) (Table 1) rises and shows the highest value for the 5Cu10Ce10Al (15.1 wt.% of CuO).

Table 2
Weight percentage Composition of the *x*Cu10Ce and *x*Cu10Ce10Al (*x* = 1; 3; 5) calcined at 600 °C; Intensity of EPR signal and copper dispersion for 1Cu10Ce; 5Cu10Ce; 1Cu10Ce10Al and 5Cu10Ce10Al.

Sample	Wt.% of CuO	Test	EPR intensity (u.a.)	Copper dispersion before test (%)
1Cu10Ce	4.42	Before	242	41
		After	127	
3Cu10Ce	12.2	Before	67	28
		After	129	
5Cu10Ce	18.77	Before	49	25
		After	133	
5%Zn5Cu10Ce	18.77	Before	–	28
		After	–	
1Cu10Ce10Al	3.4	Before	165	60
		After	42	
3Cu10Ce10Al	15.1	Before	260	80
		After	80	
5Cu10Ce10Al	15.1	Before	226	59
		After	72	
5%Zn5Cu10Ce10Al	15.1	Before	–	32
		After	–	

As for the *x*Cu10Ce catalysts, our results have shown that by increasing the copper load (Table 2) in these catalysts, the methanol conversion and the carbon assessment value are increased revealing the highest performance for the 5Cu10Ce with an optimum composition of 18.77 wt.% of CuO for dry impregnated CuO–CeO_2 without any formation of CO and CH_4.

By comparing to the *x*Cu10Ce catalysts, the *x*Cu10Ce10Al exhibit better carbon assessment (Table 1). This could be related to the influence of the alumina used with the ceria as a support in the presence of copper species knowing that the CeO_2 could oxidize carbon species by itself [18]. The comparison of these two series of catalysts (*x*Cu10Ce and *x*Cu10Ce10Al) shows that a high copper content (5Cu10Ce: 18.77 wt.% and 5Cu10Ce10Al: 15.1 wt.% of CuO) is recommended for a better catalytic activity.

After adding 5% of ZnO over 5Cu10Ce, the methanol conversion rate (99.9%) and the carbon assessment (0.99) have shown the highest values among all the tested catalysts with an amount 75% of H_2 and without any formation of CO and CH_4.

While adding 5% of ZnO over 5Cu10Ce10Al, a low CO formation is detected with absence of CH_4. Whereas comparing to the 5Cu10Ce10Al, the methanol conversion (96%) and the carbon assessment (0.73) decrease. The low carbon assessment value indicates that the addition of ZnO to xCu10Ce10Al seems to favor the carbon formation on this catalyst.

3.2. By-products formation

Over all the tested *x*Cu10Ce catalysts (Table 1), the formaldehyde (HCHO) was detected in the liquid fraction as a by-product without any formation of methyl formate. However, in the presence of mixed oxide support as for *x*Cu10Ce10Al, only the methyl formate (CH_3OCHO) was detected. Thus, the nature of the support plays a role in the formation of by-products. A rather basic support as ceria leads to the formation of formaldehyde while a rather acid support such as alumina leads to the formation of methyl formate. Takazewa, Takahashi et al. [19,20] proposed reaction pathway by nucleophilic addition of surface hydroxyls to adsorbed formaldehyde (only at high MeOH/H_2O). This attack occurs competitively to that of methoxy groups which can explain the formation of methyl formate (Table 1) observed on Al_2O_3 based support.

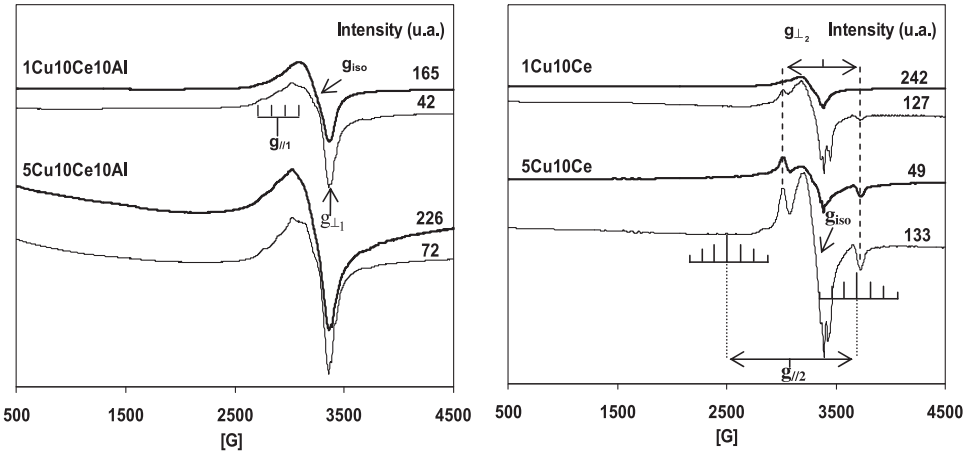

Fig. 1. EPR spectra of 1Cu10Ce; 5Cu10Ce; 1Cu10Ce10Al and 5Cu10Ce10Al before test (—) and after test (—) recorded at −196 °C.

It is also worthy to notice that, for the two types of catalysts, while increasing the copper load (Table 1), the quantity of the by-products detected in the liquid fraction drops down. Thus, the by-product formation is also directly related to the aspect of the copper load in the catalysts. This fact also points the role of copper in the reaction mechanism, probably through the adsorption of intermediate species.

The addition of Zn on the solid causes a significant decrease in the formation of by-products with the 5Cu10Ce solid or 5Cu10Ce10Al solid. The interactions between the Cu–ZnO have a significant effect on the formation of by-products and on the reaction mechanism [21].

3.3. Catalysts characterization

Several studies have shown that Electron Paramagnetic Resonance spectroscopy (EPR) is used effectively to characterize the dispersed copper (II) species in different matrix [22].

All copper based catalysts have shown an EPR spectrum characteristic of d^9-like ion with two signals of copper species (Fig. 1). The first signal with an axial symmetry having the following EPR parameters $g_{//1} = 2.323$, $g_{\perp 1} = 2.038$, $A_{//1} = 125\text{-}145$ G and $A_{\perp 1} = 27$ G and is characteristic of isolated Cu^{2+} ions [25,26]. In addition, the other signal is isotropic, centered at $g_{iso} = 2.168$ with a line width $\Delta H_{PP} = 250$ G and can be assigned to small clusters of copper ions [23–25] (Fig. 2). Our laboratory has deeply studied EPR spectra of CuCe oxide and their characteristics signals [26,27]. Table 2 shows the variation of the EPR signal intensity, calculated from normalized double integrals (DI/N) in the WINEPR program, before and after test versus the wt.% of CuO in *x*Cu10Ce and xCu10Ce10Al catalysts.

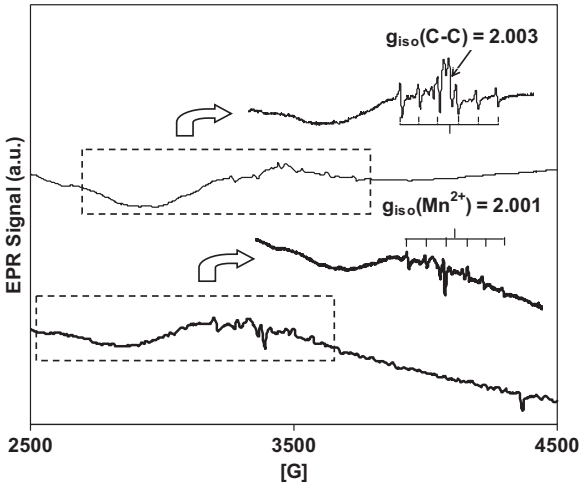

Fig. 2. EPR spectra of 10Ce10Al before test (—) and after test (—) recorded at −196 °C.

By calculating the intensity of each EPR spectrum of the *x*Cu10Ce catalysts before test, we have found that by increasing the CuO load, the intensity decreases. In fact, the intensity of the EPR signal from isolated Cu^{2+} ions is regarded as a measure of the degree of oxidation and dispersion of the catalyst [26].

The EPR spectrum of the *x*Cu10Ce also reveals the presence of seven components with relative intensities 1:2:3:4:3:2:1 of the hyperfine splitting with two identical nuclei Cu^{2+} of spin 3/2 clearly visible for the 5Cu10Ce with $g_{//2} = 2.210$, $g_{\perp 2} = 2.038$, $A_{//2} = 84$ G, and $A_{\perp 2} = 13.5$ G and situated at around 3150 G. This hyperfine structure is characteristic of the Cu^{2+} ion pairs.

Nevertheless, the formation of CuO crystallites on the catalyst surface can decrease the effective intensity of the isolated Cu^{2+} signal [26]. Thereby, the decreasing of the EPR intensities (Table 2) of 3Cu10Ce and 5Cu10Ce compared to 1Cu10Ce indicates that the number of isolated paramagnetic species in 5Cu10Ce drops down with the increase of CuO load leading to the formation of agglomerated copper species which escape EPR detection due to high dipolar interactions. Unlike 5Cu10Ce, the 1Cu10Ce presents a highly dispersed Cu^{2+} particles (41%) leading to the highest EPR intensity signal before test.

After test, reduced copper species are also revealed over the 1Cu10Ce by the decreasing of the EPR intensity (Fig. 1, Table 2). On the contrary, the EPR intensities of 3Cu10Ce and 5Cu10Ce after test increase. Thus, the intensity is also correlated with the concentration of Cu (II) species and indicating the presence of isolated Cu^{2+} species in the CeO_2 matrix. Somehow, during test, the agglomerated copper tends to be partially reduced inducing a decrease in the dipolar interactions. Thus, the silent EPR species present before test became more visible by EPR after test and leading to a higher EPR signal intensity.

In addition, these results alone indicate that the increase in methanol conversion with copper dispersion was not very significant. The comparison between the *x*Cu10Ce catalysts show that the best selectivity of H_2 obtained for 5Cu10Ce was related to the presence of large copper crystallites (25% of dispersion). The agglomerated CuO species formed during the preparation of this catalyst tend to avoid the formation of by-products which is proved by the absence of CO and CH_4 and the high carbon balance (0.96).

EPR informations of *x*Cu10Ce10Al catalysts before test are reported in Fig. 1 and Table 2. By increasing the CuO load over the 10Ce10Al support, the concentration of isolated Cu^{2+} ions increased giving a higher EPR intensity for 3Cu10Ce10Al (260) which has

the best dispersion (80%) but it decreased for 5Cu10Ce10Al (226) owning the worst dispersion (59%).

The presence of reduced species of copper after test is revealed by the decreasing intensity of EPR signal compared to that before test (Table 2).

Same to *x*Cu10Ce, the presence of less dispersed copper induces the best selectivity of H_2 with absence of CO and CH_4 which was attributed to 5Cu10Ce10Al (59%).

The addition of zinc on the catalysts does not have the same effect on the activities and the dispersions. The impregnation of Zn on 5Cu10Ce10Al causes a decrease in the methanol conversion (96%), the dispersion (32%) and the carbon assessment (0.73), besides 0.1% CO was formed. On the other hand, the impregnation of Zn on 5Cu10Ce improves the dispersion (28%), the methanol conversion (99.9%) and the carbon assessment (0.99).

There are several theories describing the nature of the interaction between Cu–ZnO, some of them consider that the major role of ZnO in a Cu based catalysts is a promoter and this role is explained by different mechanisms [28]. Furthermore, our results correlate with the theory explaining the marked effect of the interactions between Cu–ZnO on the catalytic activity due to the presence of ZnO which improves the dispersion and the reducibility of Cu^{2+} species [29]. Somehow, those interactions seem to depend directly on the nature of the support.

EPR technique can serve as a method for carbon species investigation [30,31]. Several studies have shown that carbon species and its derivatives show that an EPR signal constituted by a single line at different widths depending on the carbon species [30,31]. The EPR parameters of this signal are $g = 2.002–2.005$ and the line-width $\Delta H = 7–100$ G. The paramagnetic centers originate by mobile unpaired electrons within the carbon structure or at the surface forming free radicals. It was indicated that the EPR line-width and the unpaired spin density may be related to the surface area, the molecular structure, the particle size and defect characteristics. The increase in line-width is attributed to the formation of carbon–oxygen complexes.

Fig. 2 shows an EPR signal of 10Ce10Al after test with g_{iso}(C—C) = 2.003. This signal is isotropic, sharp with a line-width of ~6 G. The EPR parameters of this signal are consistent with localized paramagnetic spins on the carbon particles [31]. Thus, the presence of this EPR signal showing the existence of carbon species adsorbed on the 10Ce10Al support and explains the low rate of carbon (0.35).

In parallel, Fig. 2 shows an EPR six lines spectrum of high spin Mn^{2+} ions with electronic configuration $3d^5$. It has been attributed to Mn^{2+} ions ($g = 2.001$, $A = 87$ G) located in a weak axially distorted octahedral crystal field. These Mn^{2+} species are present as impurities (6 ppm) in the sample and do not have any catalytic role.

XRD patterns of 5Cu10Ce, 5%Zn5Cu10Ce, 5Cu10Ce10Al and 5%Zn5Cu10Ce10Al catalysts are shown in Fig. 3. It can be seen that fluorite type oxide structure of CeO_2 (JCPDS: 00-034-0394) is observed in all samples and remained in oxide form after test. Besides, aluminum oxide was not shown over the pattern because of its amorphous phase.

The XRD pattern of the 5Cu10Ce (Fig. 3c) catalyst before test, shows the presence of diffraction peaks related to CuO species (JCPDS: 00-045-0937) that remains even after test. After test, diffraction peaks corresponding to Cu^0 (JCPDS: 00-004-0836) were detected which signify the reduction of CuO species during test. The results of EPR confirm this fact because the intensity of EPR signal rise after test due to the dissociation of the bulk CuO which become more dispersed and detected by EPR.

After adding 5% of ZnO over 5Cu10Ce, CuO species are more visible over this catalyst before test with the presence of small diffraction peaks related to ZnO (JCPDS: 00-036-1451). After test, diffraction peaks related to CuO species disappear and Cu_2O (JCPDS: 03-065-3288) with Cu^0 (JCPDS: 00-004-0836) phase are present besides the peaks assigned to ZnO.

Thus, during test the CuO species tend to be reduced into Cu^0 and Cu^+. In their study, Pfeifer et al. [32] have shown that the high catalytic activity of the Cu/CeO_2 catalysts in the SRM reaction is directly related to the stabilization of the Cu_2O species in the presence of CeO_2. Otherwise, Reitz et al. [33], did not allocate any activity to the Cu^+ species. It is well known that the reducibility of CuO species increases when CeO_2 is used as a support or even when it is added to another mixed oxide support [34–38]. This fact could probably enhance the catalytic activity [34,37]. In our case, the higher catalytic activity of 5%Zn5Cu10Ce catalyst could be ascribed to the formation of an optimum Cu^0–Cu_2O species stabilized by chemical interaction on ceria support, and in the presence of zinc, which is in correlation with Idem and Bakhshi [11].

But this was not the case of 5%Zn5Cu10Ce10Al where the addition of 5% of ZnO has limited the formation of reduced copper species and has decreased the methanol conversion and the carbon assessment. On contrary of all other catalysts, CuO species are not detected in the pattern of 5Cu10Ce10Al solid before test. The lack of CuO peaks in these catalysts before test suggests that these particles remaining on the surface of CeO_2 may form a solid solution which escapes the XRD detection. In addition, the 5Cu10Ce10Al pattern shows the presence of $CuAl_2O_4$ (JCPDS: 00-033-0448) species. Patel and Pant [39] substantiate that the presence of alumina improves the stabilization of isolated Cu^{2+} ions in their matrix, and moderately by the formation of spinel like $CuAl_2O_4$. After test, the spinel like $CuAl_2O_4$ species becomes more identified with the presence of Cu^0 (JCPDS: 00-004-0836).

After adding 5% of ZnO over 5Cu10Ce10Al, the peaks assigned to the $CuAl_2O_4$ species are always visible without any detection of CuO and ZnO species. Unlike the 5Cu10Ce10Al, no Cu^0 is detected over the 5%Zn5Cu10Ce10Al after test showing that the reducibility of the copper in the presence of alumina is significantly affected by the addition of the zinc.

The absence of Cu^0 species in the XRD pattern of the 5%Zn5Cu10Ce10Al catalysts after test could explain the decrease of the methanol conversion and the carbon assessment values compared to the 5Cu10Ce10Al where Cu^0 species are detected. In order to understand the reducibility of copper species and the formation of Cu^0, a temperature programmed reduction study was performed on the catalysts before and after test.

TPR studies were done for the 10Ce10Al, 5Cu10Ce10Al, 5%Zn5Cu10Ce10Al, 5Cu10Ce and 5%Zn5Cu10Ce catalysts (Table 3 and Fig. 4) and the H_2 consumption calculated theoretically and measured experimentally before and after test for species that can be reduced in samples such as CeO_2, ZnO and CuO. As it is shown in Table 3 for the 10Ce10Al, ceria is not completely reduced during TPR before test (0.59 mmol g^{-1}). In fact, previous studies done in our laboratory have shown that the high load of ceria lower its dispersion over the alumina surface and diminish its reduction [40]. The TPR analysis performed after catalytic test shows that a small quantity of ceria is not reduced during test (0.27 mmol g^{-1}).

While adding copper (5Cu10Ce10Al), the reduction of ceria was kept almost the same (0.62 mmol g^{-1}) but 82% of the added copper was reduced by TPR (1.56 mmol g^{-1}). After test, TPR measurements (Fig. 4) reveal that a large part of copper was reduced during the test (difference between 1.56 and 0.73 mmol g^{-1}) showing a correlation with the decreasing intensity of the EPR signal and the presence of Cu^0 detected by XRD. The non-reduced fraction during test could be related to the $CuAl_2O_4$ stable phase detected by XRD after test.

After adding 5% of ZnO, no H_2 consumption (Table 3) or reduction peak (Fig. 4) characterizing the reduction of the ZnO species was revealed. Compared to the 5Cu10Ce10Al, the impregnation of Zn enhances the reducibility of ceria (1.34 mmol g^{-1}) but decreases

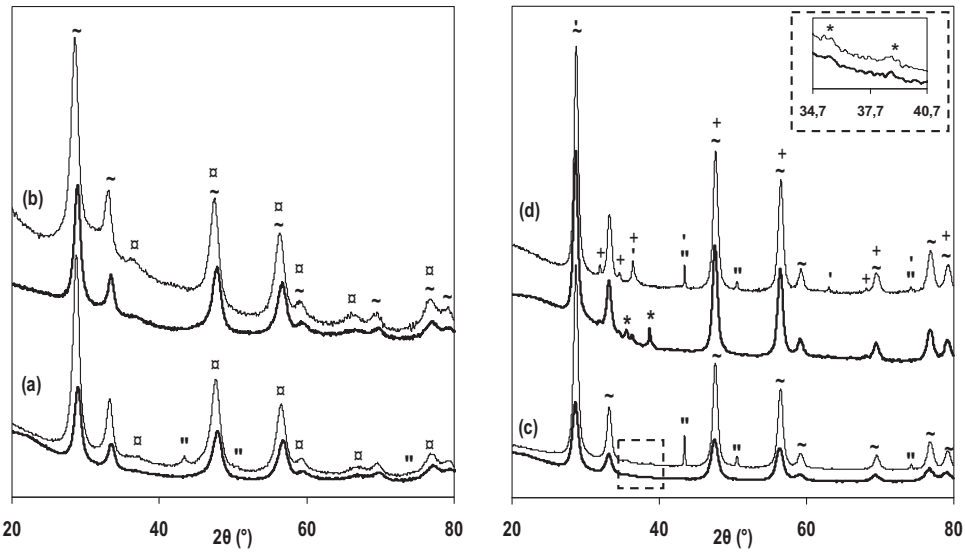

Fig. 3. XRD patterns before (—) and after test (—) for the catalysts: (a) 5Cu10Ce10Al, (b) 5%Zn5Cu10Ce10Al, (c) 5Cu10Ce and (d) 5%Zn5Cu10Ce. (∼) CeO_2 (JCPDS: 034-0394); (*) CuO (JCPDS: 045-0937); (") Cu^0 (JCPDS: 004-0836); (') Cu_2O (JCPDS: 065-3288); (+) ZnO (JCPDS: 036-1451); (¤) $CuAl_2O_4$(JCPDS: 033-0448).

Table 3
Theoretical and experimental H_2 consumption for ZnO/CuO/CeO_2 reduction before and after test for the 10Ce10Al; 5Cu10Ce10Al; 5%ZnO5Cu10Ce10Al; CeO_2; 5Cu10Ce and 5%ZnO5Cu10Ce catalysts.

	Oxide species Samples	CeO_2 10Ce10Al	CuO/CeO_2 5Cu10Ce10Al	ZnO/CuO/CeO_2 5%Zn5Cu10Ce10Al	CuO/CeO_2 5Cu10Ce	ZnO/CuO/CeO_2 5%Zn5Cu10Ce
	$[H_2]_{the}$ (mmol g^{-1})	2.20	1.90/1.90	0.61/1.90/1.90	2.36/2.36	0.61/2.36/2.36
Before test	$[H_2]_{exp}$ (mmol g^{-1})	0.59	1.56/0.62	0/0.95/1.34	2.32/2.35	0/2.16/1.19
After test	$[H_2]_{exp}$ (mmol g^{-1})	0.27	0.73/0.30	0/0.75/0.35	1.22/1.15	0/0.12/0.12

the reduction of CuO (0.95 mmol g^{-1} compared to 1.56 mmol g^{-1}). Thus, after adding 5% of ZnO, only 50% of CuO are reduced by TPR before test. This fact could be related to the $CuAl_2O_4$ spinel species detected by XRD that became more stable after adding ZnO. The addition of ZnO over the 5Cu10Ce10Al leads to lower dispersion of copper and reduction of CuO which could be the reason of the decrease of the carbon assessment value.

The H_2 consumption measured for the 5Cu10Ce after test (1.22 mmol g^{-1}) shows that 48% of CuO was reduced during test.

After adding 5% of ZnO, 91% of CuO is reduced by TPR before test (2.16 mmol g^{-1}) while 95% from them are reduced during test (0.12 mmol g^{-1}).

The reduction of ceria during the SRM test is also enhanced after adding ZnO to 5Cu10Ce (1.15 mmol g^{-1} without ZnO compared to 0.12 mmol g^{-1} with ZnO).

In this case, it seems worthy to notice that the 5%Zn5Cu10Ce has shown the highest activity, conversion rate and carbon assessment among all the tested catalysts. And unlike the other tested catalysts, its XRD pattern has shown the presence of Cu^+ and Cu^0 species. This

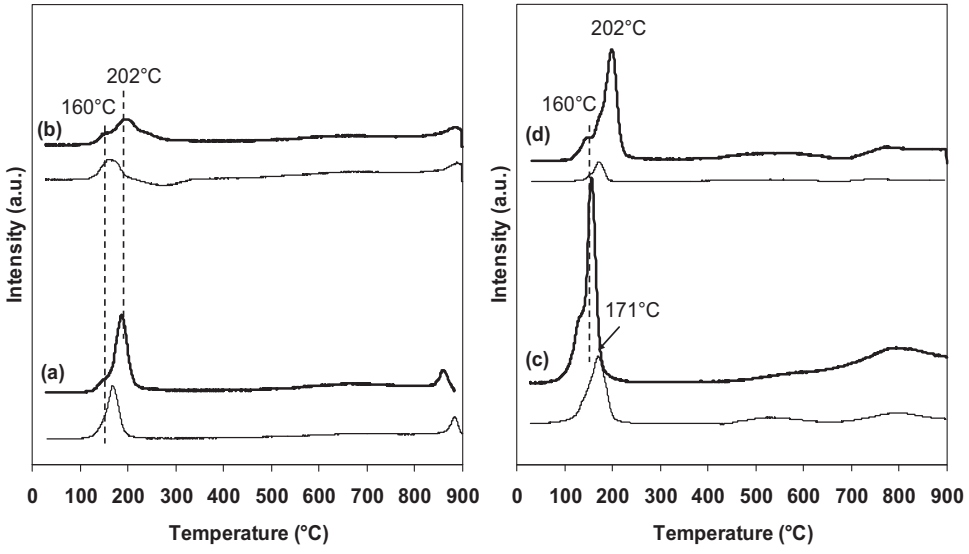

Fig. 4. TPR profiles before (—) and after test (—) for the catalysts: (a) 5Cu10Ce10Al, (b) 5%Zn5Cu10Ce10Al, (c) 5Cu10Ce and (d) 5%Zn5Cu10Ce.

proves that Ce_2O_3 plays an important role in the catalytic activity and this is in correlation with Padeste et al. [41]. Furthermore, this role is affected by the presence of an optimum of reduced copper species such as Cu^0–Cu_2O detected by XRD which gives the best catalytic performance for the 5%Zn5Cu10Ce among all the tested catalyst.

In the literature [42], the curve of the methanol conversion for the commercial catalyst (Nissan-Girdler) G66B with a weight ratio 30/60/10 ($CuO/ZnO/Al_2O_3$) is presented and shows 60% at 300 °C. Our prepared 5%Zn5Cu10Ce catalysts present 95% of conversion in the same conditions of test. With this first comparison, we can say that our catalyst 5%Zn5Cu10Ce is a good candidate for the steam reforming reaction of methanol. Further investigations should be realized as tests of stability and aging over a long period to ensure that this catalyst is equally active and stable compared to the commercial one.

4. Conclusion

Indeed, it has been shown that for *x*Cu10Ce, the best activity was attributed to 5Cu10Ce. The copper clusters are formed (5Cu10Ce), which reduces the formation of by-products during the reaction of steam reforming of methanol. This is evidenced by the disappearance of the undesired products and increasing the value of the carbon balance.

After addition of 5 wt% ZnO on 5Cu10Ce, we note that the activity, conversion and the carbon balance increase. However, our studies have shown that in presence of ZnO, Cu_2O and Cu^0 were observed, but with 5Cu10Ce, only Cu^0 species were detected after test.

The formation of an optimum Cu^+ and Cu^0 species in presence of ZnO and the action of Cu—Ce—O can explain the high activity of 5% Zn5Cu10Ce in the steam reforming reaction of methanol.

Among all the *x*Cu10Ce10Al tested catalysts, the 5Cu10Ce10Al showed the best catalytic performance in the SRM. This is related to the presence of alumina that enhances the formation of the spinels like $CuAl_2O_4$. Thus the dispersed CuO is highly reduced to active Cu^0 species during test. The dispersion is significantly affected by the addition of 5% of ZnO to 5Cu10Ce10Al. The Cu^0 species were not detected over the 5%Zn5Cu10Ce10Al after test, that explain the decrease of the methanol conversion and the carbon assessment values compared to the 5Cu10Ce10Al catalysts where Cu^0 species were detected. So, the methanol conversion rate is enhanced by the formation of an optimum Cu^0 species.

The addition of ZnO on 5Cu10Ce have promote the interaction between Cu—Ce—O leading thereafter the reduction of Cu^{2+} into Cu^+ and Cu^0 the most active species in the SRM reaction.

References

[1] F. Giorgi, F. Meleux, Geoscience 339 (2007) 721–733.
[2] G. Le Hir, G. Ramstein, Y. Donnadieu, R.T. Pierrehumbert, Geoscience 339 (2007) 274–287.
[3] M.Z. Jacobson, W.G. Colella, D. Golden, Science 3008 (24) (2005) 1901–1905.
[4] P.J. de Wild, M.J.F.M. Verhaak, Catal. Today 60 (2000) 3–10.
[5] J. Leddy, J. Fenton, Electrochem. Soc. Interface (2005) 21–23.
[6] J. Papavasiliou, G. Avgouropoulos, T. Ioannides, Catal. Commun. 6 (2005) 497–501.
[7] Y. Liu, Q. Fu, M. Flytzani-Stephanopoulos, Appl. Catal. B: Environ. 27 (2000) 179–191.
[8] M. Flytzani-Stephanopoulos, W. Liu, J. Catal. 153 (1995) 304–316.
[9] P. Fornasiero, G. Balducci, R.D. Monte, J. Kaspar, V. Sergo, G. Gubitosa, A. Ferrero, M. Graziani, J. Catal. 164 (1996) 173–183.
[10] J. Papavasiliou, G. Avgouropoulos, T. Ioannides, Catal. Commun. 5 (2004) 231–235.
[11] R.O. Idem, N.N. Bakshi, Ind. Eng. Chem. 33 (1994) 2056–2062.
[12] C.J. Jiang, D.L. Trimm, M.S. Wainwright, Appl. Catal. A: Gen. 93 (1993) 245–255.
[13] Y. Men, H. Gnaser, C. Ziegler, R. Zapf, V. Hessel, G. Kolb, Catal. Lett. 105 (2005) 35–40.
[14] J.P. Breen, J.R.H. Ross, Catal. Today 51 (1999) 521–533.
[15] E. Abi-Aad, R. Béchara, J. Grimblot, A. Aboukaïs, Chem. Mater. 5 (6) (1993) 793–797.
[16] M. Mrad, C. Gennequin, A. Aboukaïs, E. Abi-Aad, Adv. Mater. Res. 324 (2011) 157–161.
[17] M. Mrad, C. Gennequin, A. Aboukaïs, E. Abi-Aad, Catal. Today 176 (2011) 88–92.
[18] M.P. Rosynek, Catal. Rev. Sci. Eng. 16 (1977) 112–118.
[19] N. Takezawa, N. Iwasa, Catal. Today 36 (1997) 45–56.
[20] K. Takahashi, N. Takezawa, H. Kobayashi, Chem. Lett. (1985) 759–762.
[21] G. Sedmak, S. Hocevar, J. Levec, J. Catal. 213 (2003) 135–150.
[22] C. Decarne, E. Abi-Aad, B.G. Kostyuk, V.V. Lunin, A. Aboukais, Mater. Sci. 39 (2004) 2349–2354.
[23] A. Aboukaïs, A. Bennani, C.F. Aïssi, G. Wrobel, M. Guelton, J.C. Vedrine, J. Chem. Soc., Faraday Trans. 88 (1992) 615–620.
[24] A. Aboukaïs, A. Bennani, C.F. Aissi, G. Wrobel, M. Guelton, J. Chem. Soc., Faraday Trans. 88 (1992) 1321–1325.
[25] N. Takezawa, Catal. Today 37 (1995) 320–326.
[26] R. Cousin, S. Capelle, E. Abi-Aad, D. Courcot, A. Aboukaïs, Chem. Mater. 13 (2001) 3862–3870.
[27] A. Aboukais, A. Bennani, C. Lamonier-Dulongpont, E. Abi-Aad, G. Wrobel, Colloids Surf. 115 (1996) 171–177.
[28] M.M. Günter, T. Ressler, B. Bems, C. Büscher, T. Genger, O. Hinrichsen, M. Muhler, R. Schlögl, Catal. Lett. 71 (2001) 37–44.
[29] M.M. Günter, T. Ressler, R.E. Jentoft, B. Bems, J. Catal. 203 (2001) 133–149.
[30] N.D. Yordanov, S. Lubenova, S. Sokolova, Atmos. Environ. 35 (2001) 827–831.
[31] E. Abi-Aad, R. Cousin, C. Pruvost, D. Courcot, R. Noirot, C. Rigaudeau, A. Aboukaïs, Top. Catal. 16 (2001) 263–268.
[32] P. Pfeifer, K. Schubert, G. Emig, Appl. Catal. A 286 (2005) 175–185.
[33] T.L. Reitz, P.L. Lee, K.F. Czaplewski, J.C. Lang, K.E. Popp, H.H. Kung, J. Catal. 199 (2001) 193–201.
[34] C.-Y. Shiau, M.W. Ma, C.S. Chuang, Appl. Catal. A: Gen. 301 (2006) 89–95.
[35] P. Djinovic, J. Batista, J. Levec, A. Pintar, Appl. Catal. A: Gen. 364 (2009) 156–165.
[36] C.S. Polster, H. Nair, C.D. Baertsch, J. Catal. 266 (2009) 308–319.
[37] G. Avgouropoulos, T. Ioannides, H. Matralis, Appl. Catal. B: Environ. 56 (2005) 87–93.
[38] G. Busca, J. Lamotte, J.C. Lavalley, V. Lorenzelli, J. Am. Chem. Soc. 109 (1987) 5197–5205.
[39] S. Patel, K.K. Pant, Fuel Process. Technol. 88 (2007) 825–832.
[40] M.N. Bokova, C. Decarne, E. Abi-Aad, A.N. Pryakhin, V.V. Lunin, A. Aboukaïs, Thermochim. Acta 428 (2005) 165–171.
[41] C. Padeste, N. Cant, D.L. Trimm, Catal. Lett. 24 (1994) 95–105.
[42] G. Huang, B.-J. Liaw, C.-J. Jhang, Y.-Z. Chen, Appl. Catal. A: Gen. 358 (2009) 7–12.